MECHANIKA TEORETYCZNA
I STOSOWANA
Journal of Theoretical
and Applied Mechanics
2, 35, 1997

A TIME-MARCHING METHODS FOR CALCULATION OF THE WATER VAPOR FLOWS

TADUESZ CHMIELNIAK

WŁODZIMIERZ WRÓBLEWSKI

SŁAWOMIR DYKAS

Institute of Power Machinery, Silesian Technical University

e-mail: wroblews@zeus.polsl.gliwice.pl

A two-dimensional Euler code is developed for predicting the flowfield of water vapor in turbomachinery channels. The empirical equation of state given by Rivkin and Kremenevskaya (1967) is chosen for estimating the water vapor properties. The governing equations are discretized by the cell-centered finite volume formulation. The numerical procedure is based on an explicit Godunov-type scheme using the exact Riemann solver for the real gas.

Key words: Euler equations, water vapor, upwind scheme, Riemann problem

1. Introduction

Numerical computation methods based upon the Riemann problem (Godunov-type methods) have met a marked favour during the last decade, mainly through the emergence of high-resolution upwind methods, which make use of the basic concepts introduced by Godunov (1959) and Van Leer (1979). The finite-volume formulation of these methods has led to the development of powerful codes, which have allowed us to solve a number of problems involving a complex turbomachinery geometry. The comparison of four Godunov-type methods and one of the Flux Vector Splitting methods for solution of the perfect gas flow was presented by Chmielniak et al. (995).

In this paper there are presented two methods of approach to the equilibrium water vapor flow calculations. In the first one, the behaviour of the

water vapor is approximated by the perfect gas equation of state with an "equivalent" gas constant and isentropic exponent. In the second method all properties of steam on the both sides of the saturation line are computed from the empirical equations proposed by Rivkin and Kremenevskaya (1967).

Because of the computational speed and difficulties in coding the first method is more popular and widely used. The main problem of this work is to find differences between both these methods and to show the advantages and disadvantages of each of them.

In the second part of this paper the method of solution and results of computations of the non-equilibrium wet steam flow is described. The technique of calculation is based on the first of the above mentioned methods for the equilibrium single-phase flows including with the nucleation and droplet growth processes.

2. Governing equations

The two-dimensional flow of the water vapor is described by the Euler equation written in the following divergence form

$$\frac{\partial \boldsymbol{Q}}{\partial t} + \frac{\partial \boldsymbol{F}}{\partial x} + \frac{\partial \boldsymbol{G}}{\partial y} = \boldsymbol{0} \tag{2.1}$$

where

$$\boldsymbol{Q} = \begin{bmatrix} \rho \\ \rho u \\ \rho v \\ e \end{bmatrix} \qquad \boldsymbol{F} = \begin{bmatrix} \rho u \\ \rho u^2 + p \\ \rho uv \\ u(e+p) \end{bmatrix} \qquad \boldsymbol{G} = \begin{bmatrix} \rho v \\ \rho uv \\ \rho v^2 + p \\ v(e+p) \end{bmatrix}$$

and ρ, p, e – density, pressure and energy per unit.

If we deal with a perfect gas equation of state the value of energy e is calculated as

$$e = \frac{p}{\gamma - 1} + \frac{1}{2}\rho(u^2 + v^2)$$

where γ is the isentropic exponent. The value of pressure p at each iteration step is calculated from the relation

$$p = (\gamma - 1)\left[e - \frac{1}{2}\rho(u^2 + v^2)\right]$$

When using the real gas equation of state the energy is calculated from the relation

$$e = h\rho - p + \frac{1}{2}\rho(u^2 + v^2)$$

where h is the enthalpy of water vapor calculated from the relation proposed by Rivkin and Kremenevskaya (1967).

The pressure is calculated from the non-linear equation using the Newton iteration process

$$p = h(p, \rho)\rho - e + \frac{1}{2}\rho(u^2 + v^2)$$

3. Homogenous nucleation

The non-equlibrium calculation of the water vapor expansion flow is based on the classical theory of condensation by homogenous nucleation. In the zones where the flow is nucleating or wet, equations (2.1) have to be satisfied simultaneously with the equations describing nucleation and droplet growth.

Condensation on a liquid droplet proceeds at a rate governed by the ability of the vapor to conduct the latent heat L away from the droplet surface. The generally accepted form of the droplet growth equation is that due to Gyarmathy (1960), which takes into account the diffusion of vapor molecules through a surrounding gas as well as heat and mass transfer, and the influence of capillarity

$$\frac{\partial r}{\partial t} = \frac{\lambda}{(r + 1.59 l_s)\rho_l} \frac{T_l - T_g}{h_g - h_l} \tag{3.1}$$

where

ρ, T_l, h_l, ρ_l – radius, temperature, enthalpy and density, respectively, of droplets of the ith group

λ, T_g, h_g – thermal conductivity, temperature and enthalpy, respectively, of the vapor

l_s – free path of the group of droplets

dr/dt – time derivative following a particular droplet.

4. Numerical algorithm

The algorithm used to solve the system of equations (2.1) and (3.1) is a time-marching Godunov-type method (cf Chmielniak and Wróblewski (1995),

Godunov (1959), Hirsch (1990)). The discretisation in space of the flow gradients was carried out using the cell-centered finite volume method. The explicit, the first order accuracy in time integration is implemented.

Integration in space

The values of numerical fluxes on the surfaces bounding the calculation cell were solutions of the local one-dimensional Riemann problems. This method requires:

- Defining the discrete (piecewise constant) values of conservative variables for the time level t^n on each cell surface necessary to formulate the local Riemann problems
- Solution of the one-dimensional Riemann problem for the direction normal to the interface of cell
- Calculation of the numerical fluxes on the cell boundaries and obtaining the averaged solution in time t^{n+1}.

High order accuracy in space

The classical Godunov scheme leads to monotonic algorithms of the first order accuracy in space. To obtain higher accuracy preserving monotonicity, the van Leer MUSCL approximation has been applied (cf Hirsch (1990), van Leer (1979)) with the van Albada limiter function s (cf van Albada et al. (1982)). In this case, the vector of conservative variables is computed from the equation

$$\begin{aligned} U^L_{i+1/2} &= U_i + \left[\frac{s}{4}\Big((1-ks)\nabla_\xi U + (1+ks)\Delta_\xi U\Big)\right]_i \\ U^R_{i+1/2} &= U_{i+1} + \left[\frac{s}{4}\Big((1-ks)\Delta_\xi U + (1+ks)\nabla_\xi U\Big)\right]_{i+1} \end{aligned} \tag{4.1}$$

where

$$\Delta_\xi U = U_{i+1} - U_i \qquad \nabla_\xi U = U_i - U_{i-1}$$

$$s = \frac{2\Delta_\xi U \nabla_\xi U + \varepsilon}{(\Delta_\xi U)^2 + (\nabla_\xi U)^2 + \varepsilon}$$

The value ε was introduced to avoid division by zero ($\varepsilon = 10^{-5}$). For $k = 1/3$ we obtain the third order accuracy scheme. With the use of the flux limiter the scheme shows properties, which are similar to those of the TVD-schemes.

5. The exact Riemann solver for the real gas equation of state

In the case when the water vapor is described by the real gas equation of state only the exact Riemann solver is applied calculation of the fluxes at the cell boundaries.

Riemann's viewpoint consists in assuming that at every point within the flowfield, any variation will engender a couple of waves, facing to the right and to the left respectively. Connection between the two domains (l^*, r^*) takes place across the contact surface (Fig.1).

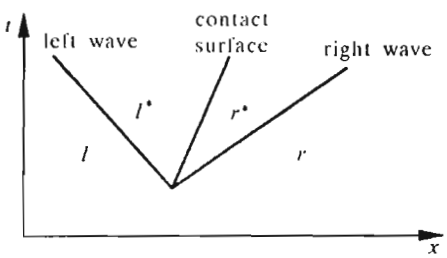

Fig. 1. Representation of the Riemann problem of gas dynamics

The strategy of resolution of this problem consists in giving a value for the pressure in the region between the right and left facing waves: $p^* = p_l^* = p_r^*$. Knowing this pressure, one determines directly the type of each wave. To determine the flow parameters behind the waves (r^* and l^* states), one has to know the jump conditions across each type of the wave:

— *Riemann invariants* for rarefaction waves

$$w_1 = s \qquad w_2 = u \pm \int_\rho \frac{c(\rho, s)}{\rho}\, d\rho \tag{5.1}$$

where for the perfect gas they have a form $w_1 = s$, $w_2 = u \pm \frac{2}{\gamma-1}c$ (c denotes the speed of sound);

— *governing equations* for the shock waves (Hugoniot relations for the perfect gas)

$$\begin{aligned}
&\rho_i D - \rho_i u_i = \rho_i^* D - \rho_i^* u_i^* \\
&\rho_i u_i D - (p_i + \rho_i u_i^2) = \rho_i^* u_i^* D - (p_i^* + \rho_i^* u_i^{*2}) \\
&e_i D - u_i(e_i + p_i) = e_i^* D - u_i^*(e_i^* + p_i^*)
\end{aligned} \tag{5.2}$$

where D is the actual propagation velocity of the shock wave, i denotes the state l or r and across the contact surface the pressure p^* and velocity u^* are constant.

The main difficulty for the real gas equation of state is to integrate the Riemann invariant

$$u_i^* = u_i \pm \int_{\rho_i}^{\rho_i^*} \frac{c(\rho, s)}{\rho}\, d\rho$$

The first difficulty lies in finding the upper limit of the Riemann invariant integral and then in numerical solving of it. The upper limit can be obtained from the condition of unchanged entropy across the rarefaction wave solving non-linear equation

$$s(p_i, \rho_i) = s(p_i^*, \rho_i^*)$$

Knowing the both limits the value of the integral is computed numerically along the isentrope curve.

The procedure for solving the Riemann problem for a real gas is exhaustively described by Saurel et al. (1994).

6. Numerical results

Some selected problems of the equilibrium and non-equilibrium expansion flow of the water vapor were tested. In the first test a comparison between the flows of the water vapor defined as a perfect gas and the water vapor defined as a real gas, respectively, is done. In the second test there are shown the computational results of water vapor flow with rapid nucleation.

6.1. Equilibrium flow

Three flow problems are selected to test performance of the water vapor flow. The water vapor flow with the perfect gas equation of state was calculated for the constant isenpropic exponent $\gamma = 1.3$. The numerical tests presented below are very popular and widely described in literature. All the results are obtained with the 2D code. The first classical, 1D Sod test is used to investigate the solution accuracy for one-dimensional wave structure. In the second problem the capabilities of the schemes for resolution of the complex

intersection wave structure for a channel flow over a bump are analysed. In the third test a flow trough a Laval nozzle is investigated.

6.1.1. Sod's problem

This is so called Sod's problem (cf Sod (1978)); this is a very mild test and its solution consist of left rarefaction, contact and right shock. This test has started with the following initial values

$$\rho_L = 1.25 \qquad u_L = 0.0 \qquad p_L = 3.0$$
$$\rho_R = 0.333 \qquad u_R = 0.0 \qquad p_R = 0.5$$

The computation are done for the first order accuracy scheme in space with $CFL = 0.7$. The computational results are compared with the known exact analytical solution of this problem for a perfect gas (Fig.2).

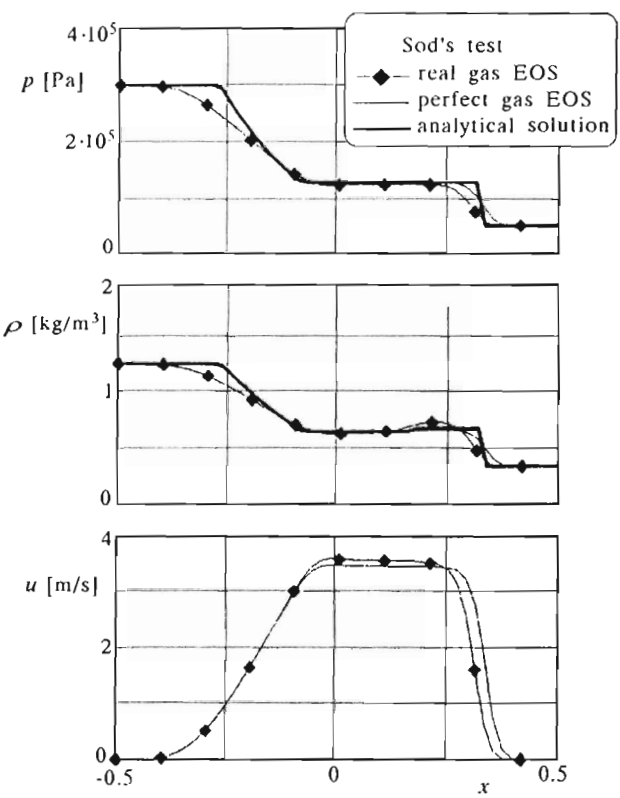

Fig. 2. Pressure, density and velocity distribution for Sod's test

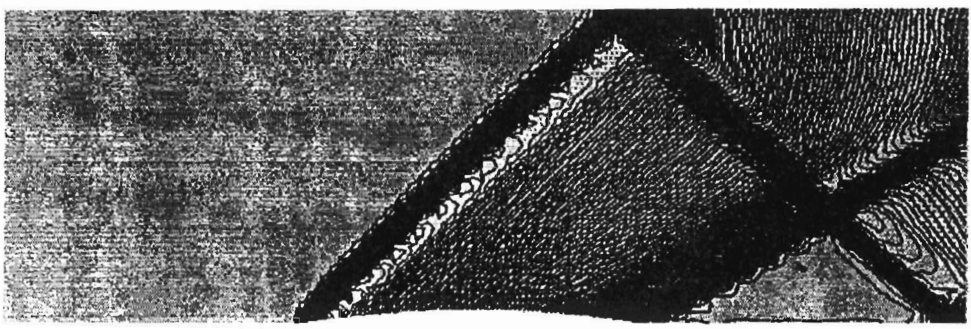

Fig. 3. The geometry and the pressure contours

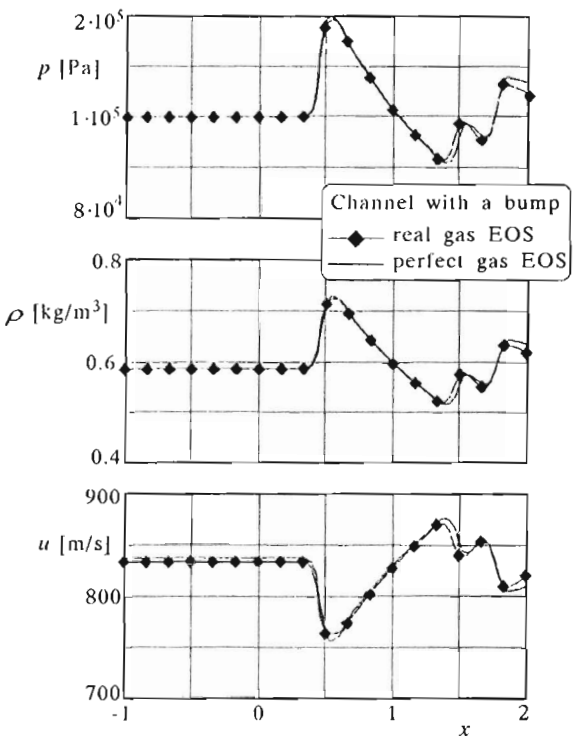

Fig. 4. Pressure, density and velocity distributions for a middle section ($y = 0.5$)

For the third order accuracy scheme in space the differences between the discussed methods almost disappear.

6.1.2. Channel flow over a bump

A channel flow over a bump is a standard test case proposed by Rizzi and Viviand (1981). In this test the supersonic flow with the inlet Mach number Ma = 1.6 considered. To the calculation the "H" non-ortogonal numerical grid (91 × 41) was chosen. The geometry of the channel and the pressure contours are shown in Fig.3. The bump the thickness ratio equals 4%.

The results are obtained for the third order accuracy in space. In Fig.4 the pressure, density end velocity distributions along the section $y = 0.5$ are compared.

Small differences between the flow parameters across the oblique shock waves along the middle section (Fig.4) are observed.

6.1.3. The Laval nozzle

The geometry of the Laval nozzle with Witoszynski's geometry (cf Orzechowski (1964)) was chosen. The "H" non-ortogonal grid (91 × 41) was adopted. For this test the following inlet parameters were used: total pressure $p_0 = 1$ bar and total density $\rho_0 = 0.5\,\mathrm{kg/m^3}$. The outlet pressure was $p_{out} = 0.1$ bar.

The third order accuracy in the 3D scheme was used. In this case are compared the pressure, density end velocity distributions along the middle section for the water vapor and perfect gas models, respectively (Fig.5). The differences appear only in the outlet area of the nozzle, because of the high value of velocity.

In this test the distribution of the thermodynamic parameters (enthalpy, entropy, dryness fraction) of the water vapor for the real gas model during the expansion flow trough the Laval nozzle with Witoszynski's geometry (cf Orzechowski (1964)), Fig.6, are presented, Fig.7. The values of these parameters calculated with the perfect gas model with constant γ are not physical.

6.2. Non-equlibrium flow

For the test computations the Laval nozzle (Fig.9) and the turbine cascade section (Fig.11) were chosen. Two-dimensional computations for the Laval nozzle with the literature computations and the experiment given by Bakhtar

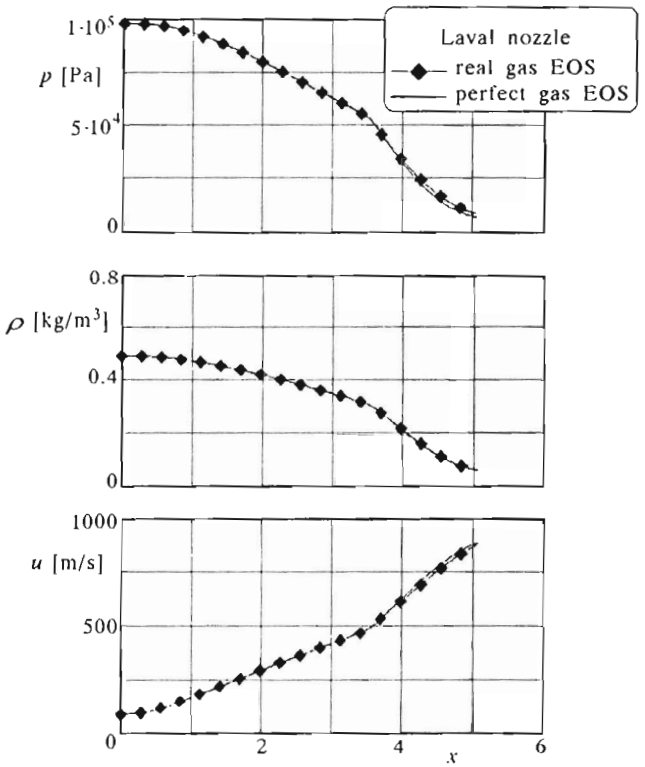

Fig. 5. Pressure, density and velocity distributions for a middle section

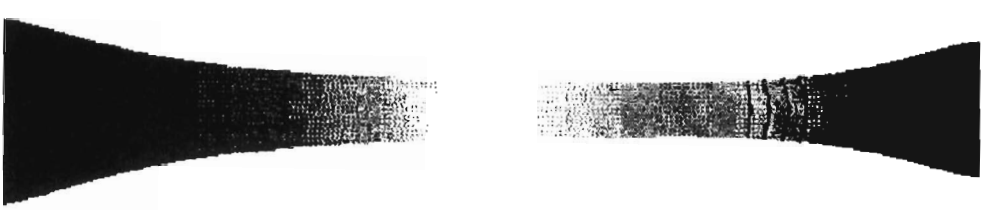

Fig. 6. Geometry and the wetness fraction contours ($w > 0$)

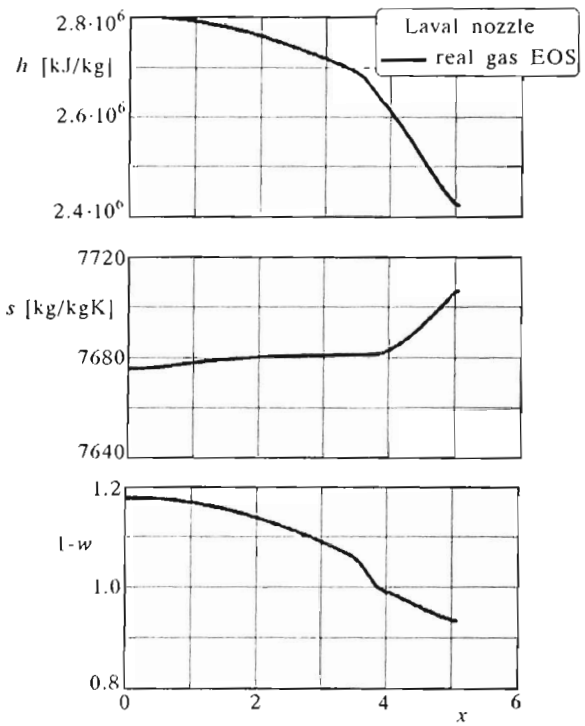

Fig. 7. Enthalpy, entropy and dryness fractions distribution for a middle section

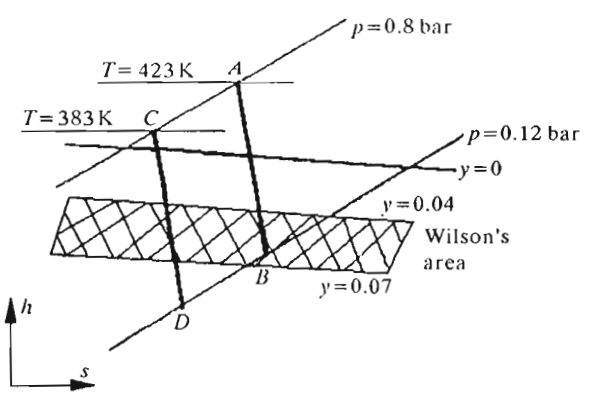

Fig. 8. Expansion lines for two initial data

and Tochai (1980) were compared. The effect of the inlet parameters, as well as the location and quantity of nucleation was tested.

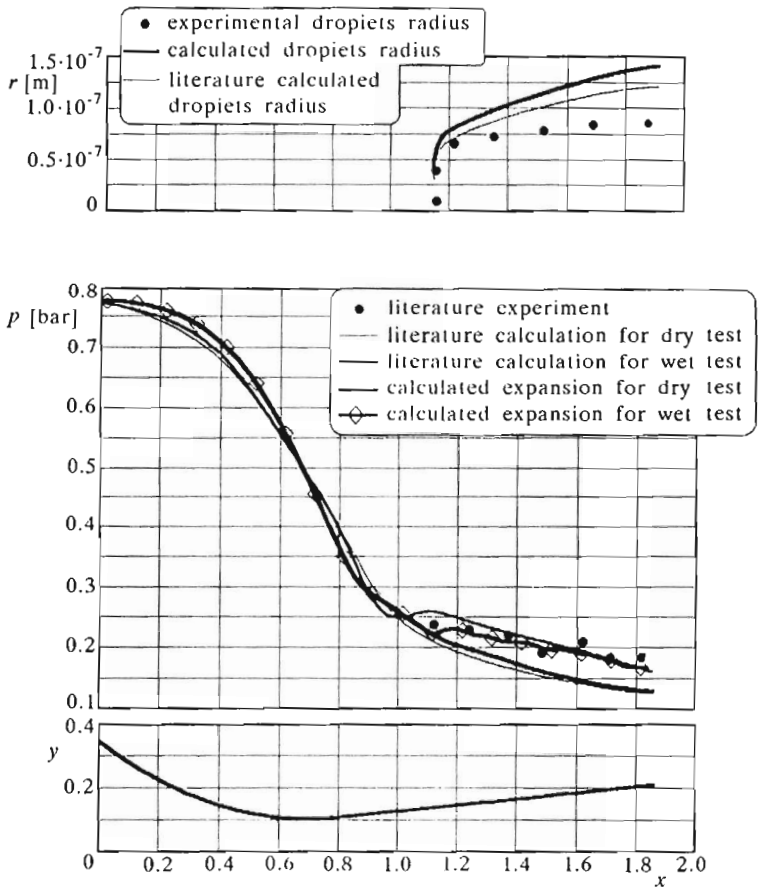

Fig. 9. Geometry, pressure and droplets radius distributions for the Laval nozzle. Comparison with the literature results

6.2.1. The Laval nozzle

Nozzle computations were done for: inlet pressure $p_0 = 0.8$ bar, outlet pressure $p_{out} = 0.12$ bar and two inlet temperatures, 383 K and 423 K, Fig.8.

Fig.3 shows the comparison of pressure and droplets radius distributions for the middle intersections of the Laval nozzle with the literature results. The beginning and the quantity of the rapid nucleation is close to the experiment and literature calculation (cf Bakhtar and Tochai (1980)).

Fig.10 shows the effect of the inlet parameters and location of rapid nucleation. There were compared the pressure distributions along the middle intersection lines for two expansions. The departure of the pressure from the equilibrium state for both expansions in Fig.10 began in Wilson's area.

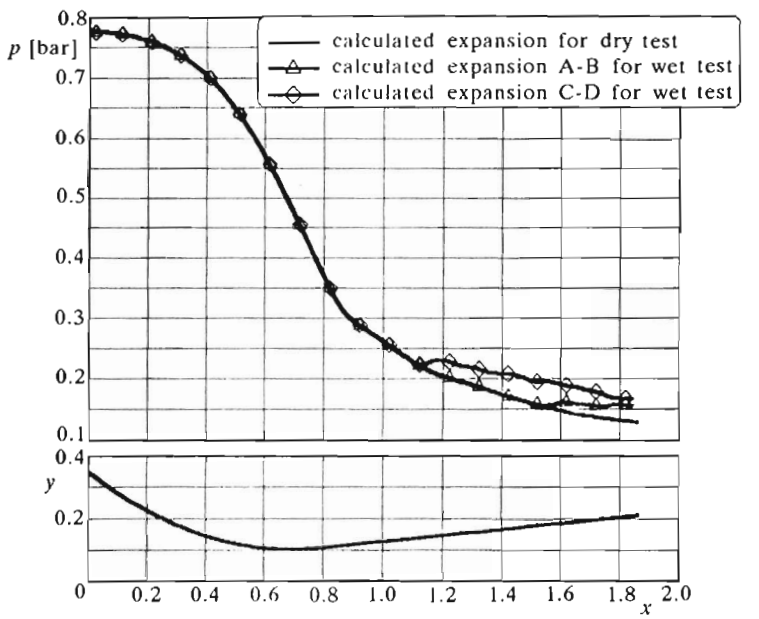

Fig. 10. Geometry and pressure distributions for the Laval nozzle. Influence of the inlet parameters

6.2.2. The turbine cascade

The calculations of the nucleating flow trough a turbine stator were done for the same inlet and outlet parameters as the calculation for the Laval nozzle (Fig.9). For calculation the "H" non-ortogonal computational grid was used. The location of the liquid phase is conformable to Wilson's area.

We can observe in an increase in the static pressure above the corresponding values of the superheated steam when the condensation occurs (Fig.12).

Fig.13 shows the wetness rate distribution, Wilson's area is located close to the trailing edge where the departure of flow parameters from the equilibrium state is initiated (Fig.12).

In non-equlibrium tests the losses in efficiency for the nozzle and turbine cascade were estimated.

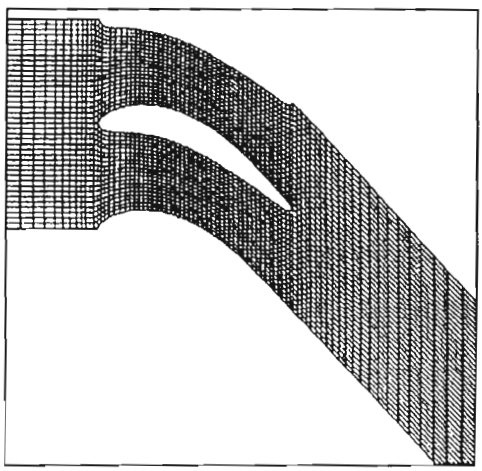

Fig. 11. Geometry of the turbine cascade

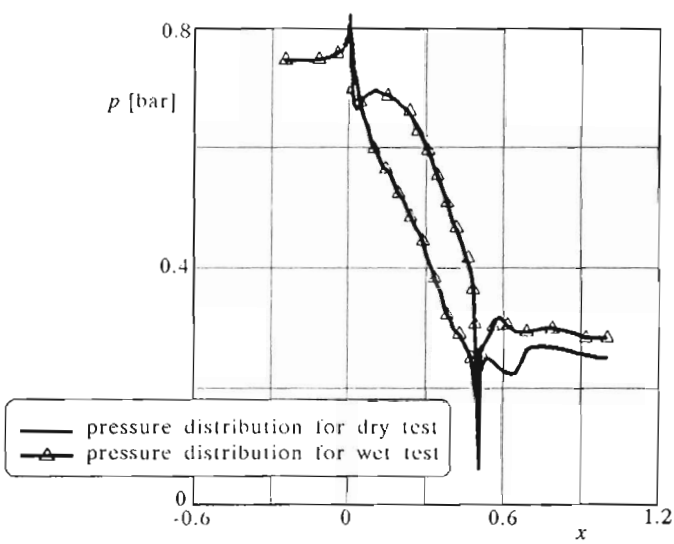

Fig. 12. Pressure distribution for a turbine cascade along the $\eta = 0$ and $\eta = \eta_{max}$ lines

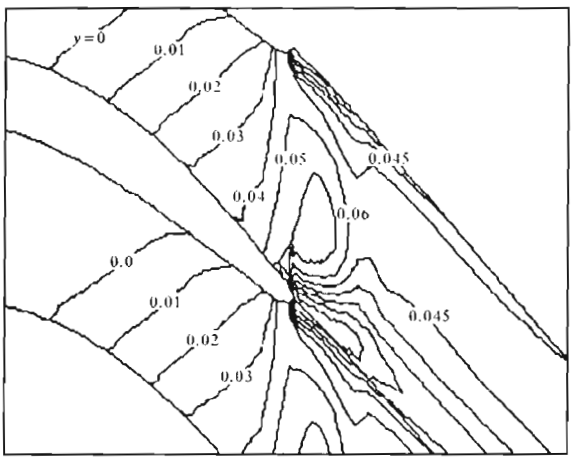

Fig. 13. Distribution of the wetness fraction

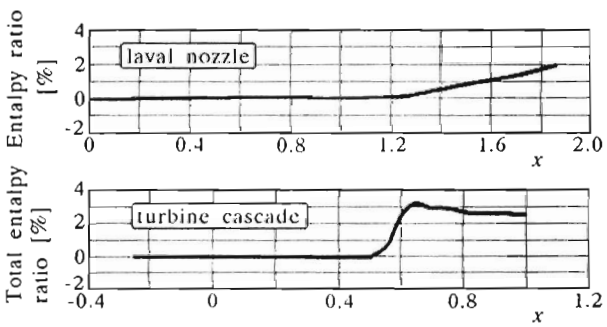

Fig. 14. Relative change of total enthalpy for Laval nozzle and turbine cascade

In Fig.14 the losses in total enthalpy when the rapid nucleation appears were estimated using the relation

$$\Delta h = \frac{h_{tot} - h_{tot}^{con}}{h_{tot}}$$

where h_{tot} represents the total enthalpy without condensation and h_{tot}^{con} represents the total enthalpy with spontaneous condensation. In both cases we have dealt with supersonic outlet. For the flow through the Laval nozzle the losses in total enthalpy in the outlet area equaled more than 2% and for the turbine cascade more than 3%.

7. Conclusions

The method based on the real gas equation of state is uncomparable much more time-consuming than the method based on the perfect gas equation of state, mostly because of many iteration processes needed. The tests showed the differences in the flow variables, mostly significant differences in the values of velocity obtained by means of these methods. A physical nature of the flow for an algorithm with real gas equation of state is preserved (it is clearly showed in the second test). The algorithm based on the perfect gas equation of state with $\gamma = 1.3$ gives approximate values of the water vapor parameters and false values of the thermodynamic functions. Using the real gas equations when calculating the water vapor expansion all thermodynamic variables can be estimated with a high accuracy in relation to the real physical phenomena.

Using the perfect gas equation of state with constant isentropic exponent and the gas constant we cannot describe the properties of the water vapor expansion flow. Otherwise, this way we cannot calculate precisely the enthalpy, entropy and other thermodynamic values. Therefore we have to use an equivalent isentropic exponent and the gas constant. It is relatively inconvenient and a little artificial. Using the real gas equation of state all thermodynamic variables for the water vapor are directly obtained, but it is a very time-consuming process. However for the fast computer it is not so important.

For the non-equlibrium tests the comparison of calculated results for the Laval nozzle with the literature data (both theoretical and experimental), Bakhart et al. (1980), gives satisfactory results. Similarly the turbine cascade calculations gave good results of the location and quantity of rapid nucleation. In spite the fact that not all complicated physical phenomena appearing in wet steam flow were taken into consideration in the present algorithm the results obtained are correct.

A high stability and convergence of this scheme make possible the calculations for wide range of parameters.

References

1. VAN ALBADA G.D., VAN LEER B., ROBERTS W.W., 1982, A Comparative Study of Computational Methods in Cosmic Gas Dynamics, *Astron. Astrophysics*, **108**, 76-84

2. BAKHART F., MOHAMMADI TOCHAI M.T., 1980, An Investigation of Two-Dimensional Flows of Nucleating and Wet Steam by the Time-Marching Method, *Int. J. Heat and Fluid Flow*, **2**, 1

3. CHMIELNIAK T.J., WRÓBLEWSKI W., 1995, Application of High Accuracy Upwind Schemes to Numerical Solution of Transonic Flows in Turbomachinery Blade Passages, *VDI-Berichte*, **1185**, 63-77

4. CHMIELNIAK T.J., WRÓBLEWSKI W., DYKAS S., 1995, Comparison of the Godunov-type Methods Using for Transonic Internal Flow Computotions, *Cieplne maszyny Przeplywowe*, **108**, 89-98 (in Poland)

5. DEJC M.E., 1981, *Gasdynamic of Two-Phase Flow*, Moscow, (in Russian)

6. GODUNOV S.K., 1959, A Difference Scheme for Numerical Computation of Discontinuous Solution of Hydrodynamic Equations, *Math. Sbornik*, **47**, 271-306 (in Russian)

7. GYARMATHY G., 1960, *Grundlagen einer Theorie der Nassdampfturbine*, Juris Verlag, Zürich

8. HIRSCH C., 1990, *Numerical Computation of Internal and External Flows*, John Wiley and Sons, Chichester

9. KONTROWITZ A., 1951, Nucleation in Very Rapid Vapor Expansions, *Journal Chem. Phys.*, **19**, 1097-1100

10. KRÓL T., 1971, Results of Optical Measurements of Diameters of Drops Formed due to Condensations of the Steam in de Laval Nozzle, *Prace IMP*, **57**, (in Polish)

11. VAN LEER B., 1979, Towards the Ultimate Conservative Difference Scheme. V.A. Second Order Sequel to Godunov's method, *Journal of Computational Physics*, **32**, 101-136

12. ORZECHOWSKI M., 1964, *Fluid Mechanics*, Skrypt Politechniki Łódzkiej, Łódź

13. RIVKIN C.L., KREMENEVSKAYA E.A., 1967, Equations of State of Water and Water Vapor, *Teploenergetika*, **3**, 69-73, (in Russia)

14. RIZZI A.W., VIVIAND H., 1981, Numerical Methods for the Computations of Transonic Flows with Shock Waves, *Notes on Numerical Fluid Mechanics*, **3**, Vieweg, Braunschweig

15. SAUREL R., LAURINI M., LORAND J.C., 1994, Exact amd Approximate Riemann Solver for Real Gases, *Journal of Computational Phisics*, **112**, 126-137

16. SOD G.A., 1978, A Survey of Several Finite Difference Methods for Systems of Non-linear Hyperbolic Conservation Laws, *J. Comput. Physics*, **27**, 1-31

Metoda kroków czasowych w obliczeniach przepływu pary wodnej

Streszczenie

W niniejszej pracy przedstawiono obliczenia dwuwymiarowego równowagowego i nierównowagowego przeplywu pary wodnej. Obliczenia bazują na metodzie kroków czasowych rozwiązania równania Eulera. Dla równowagowego przepływu porównano rozkłady parametrów pola przeplywu w przypadku zastosowania równania stanu gazu rzeczywistego z przypadkiem użycia równania stanu gazu doskonalego. Metodyka obliczń przeplywu nierównowagowego oparta jest na równoczesnym rozwiązywaniu

cząstkowych równań różniczkowych Eulera oraz dodatkowego równania zachowania, jakim jest równanie wzrostu kropli, wiążącego sobą zjawiska wymiany masy i energii pomiędzy fazą gazową a ciekłą. Do rozwiązania równań zachowania wykorzystano metodę objętości skończonych przy zastosowaniu do dyskretyzaji obszaru obliczeniowego siatki regularnej typu "H". Do wyznaczenia strumieni bilansowych na granicach komórek obliczeniowych użyto schematu upwind wyższego rzędu dokładności w przestrzeni. Wyniki obliczeń przedstawiono dla geometrii dyszy de Lavala oraz kanału łopatkowego turbiny.

Manuscript received October 10, 1996; accepted for print January 10, 1997